Volume 18, Number 3, 2025. pp. 309-317

Jordan Journal of Physics

ARTICLE

Optimization of the Third Electrode Design in Electrostatic Einzel Lenses

Alaa A. H. Ahmad[a], **Abdullah I. M. Alabdullah**[a] and **Mohammed A. Hussein**[b]

[a] *Department of physics, College of Sciences, University of Mosul, Mosul, Iraq.*
[b] *College of Education for Women, University of Kirkuk, Kirkuk, Iraq.*

Doi: **https://doi.org/10.47011/18.3.5**

Received on: 10/01/2024; *Accepted on: 22/07/2024*

Abstract: In this study, we designed an electrostatic Einzel lens with three electrodes. The two electrodes at each end were set to the ground potential, while a positive potential was applied to the central electrode. We explored the impact of changing the geometry of the third electrode on the trajectory of paraxial electron beams and the two-dimensional emittance. Notably, altering the outer diameter of the third electrode while keeping other parameters constant had a clear effect on the equipotential surface. This modification improved the electric potential and electric field distribution within the lens, resulting in enhancements in beam emittance of approximately 73% and a reduction in the cross-over radius of the paraxial trajectory by 27%. Moreover, we introduced a cylindrical shape for the third electrode, acting as a cover for the first and second electrodes. Investigating its length revealed further enhancements in the path of the paraxial beam of electrons by 37% and reduced beam emittance by 76%. These findings highlight the importance of optimizing the third electrode's design to achieve superior performance in charged particle optics applications. The study demonstrates the potential of employing novel geometries and configurations to enhance the overall efficiency of electrostatic Einzel lenses.

Keywords: Electrostatic lenses, Einzel lens, Ion beam focusing, Particle optics, Third electrode, Outer radius, Length.

1. Introduction

Electrostatic lenses are used for various purposes, as acceleration of both electron and ion rays. The theoretical framework for electrostatic lenses was developed between 1930 and 1955. In many instances, the ion optics featuring electrostatic lenses is commonly referred to as electron optics. These electrostatic lenses have a substantial impact on the design of low-energy electrostatic accelerators, such as the Cockcroft–Walton and Van de Graaff accelerators, which are widely used for preparing low-energy electron and ion beams for experiments involving the scattering of particles. Some storage rings have been created with exclusive use of electrostatic deflection and focusing devices [1]. Another significant application of the electrostatic lens is in the design of a hemispherical energy analyzer, a device intended to examine the kinetic energy of electrons across different energy levels. Energy analyzers are one of the most important and most used electrostatic analyzers at the present time [2]. The geometry of the electrodes is critical to the performance of electrostatic lenses, as it directly affects the electron beam diameter at the image plane and enables precise control of beam

Corresponding Author: Alaa A. H. Ahmad **Email**: alaahakeim@uomosul.edu.iq

acceleration and deceleration. The electrostatic lens is essential to the development of cutting-edge technologies in various fields, including electron and ion beam systems, particle accelerators, and advanced microscopy [3]. Electrostatic lenses are also employed in compound lenses (magnetic-electric), which enhance optical performance and increase the resolving power of objective lenses in scanning transmission electron microscopes (STEM) [4].

An Einzel lens, also known as a unipotential lens, is an electrostatic lens for charged particles, designed to focus the particles while preserving their initial energy. It comprises a series of three or more cylindrical or rectangular apertures, or tubes, arranged in line with a central axis. In ion optics, the purpose of the Einzel lens is to focus ions in flight by manipulating the electric field along their path [5]. The symmetry of the electrostatic potential inside the lens ensures that the particles (electrons and ions) maintain their initial energy upon exiting the lens. However, the velocity of outer particles is adjusted in a manner that leads them to converge toward the axis, resulting in a slight delay in their arrival at the focal point compared to particles traveling along a straight path [6]. This phenomenon can be observed in Fig. 1.

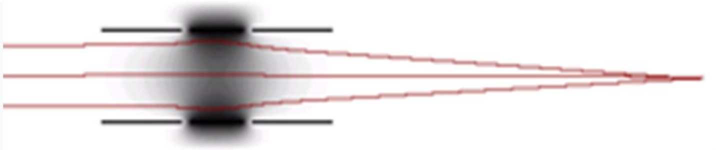

FIG. 1. A perspective view of an Einzel lens.

The formula describing the alteration in radial velocity for a particle as it transitions between any two cylinders within the lens is as follows:

$$\Delta v_r = \int \frac{GE_r(r,z)}{Mv_z} dz \qquad (1)$$

Here, the z-axis runs through the center of the lens, and (r) represents the direction perpendicular to the z-axis. In the case when the lens is constructed using cylindrical electrodes, the electric field is uniform and symmetrical with respect to the z-axis. E_r (r, z) represents the radial component of the electric field, M denotes the mass of the particle traveling through the field, v_r is the particle's velocity, and G is its charge. The integral is computed over the region between the polepieces, which is where the focusing effects of the lens occur. The dual poles (or plates) function as an electrostatic immersion lens, and as a result, an Einzel lens can be described as two or more such electrostatic immersion lenses combined. To select the focal length of the lens, one can apply Eq. (1) twice for each set of poles (plates) [7].

The concept of the beam emittance parameter has been introduced as a key parameter for evaluating beam quality. Emittance, similar to brightness, represents a characteristic of electron beams that offers important information about their propagation characteristics [8]:

$$r'' = \frac{\varepsilon^2}{r^3} = \frac{\varepsilon_n^2}{\gamma^2\beta^2 r^3} \qquad (2)$$

where ε is the emittance, β is the beam brightness, and γ is the transport parameter.

Beams exhibiting random variations in their transverse velocities display a divergence in angle concerning the propagation axis. This angular spread places constraints on the ability to effectively focus such beams. So, emittance is a gauge of a beam's parallelism and the evaluation of beam quality for various applications. [9].

The current research seeks to discover the optimal genesis for an electrostatic Einzel lens that improves the electron beam path and emittance. In this inquiry, we have taken significant strides in designing a variety of electrostatic lenses with remarkable performance enhancements. This study explores key parameters, including the outer diameter, length of the third electrode, and the electron path within the third electrode. Significant improvements were achieved, including reduced beam emittance and a minimized cross-over radius of the paraxial trajectory.

In this study, the suggested lens was designed using SIMION 8.0 software. Calculation included the axial field, potential distribution, equipotential lines, and a LUA program to identify the trajectory of the electron beam and emittance parameters. SIMION 8.0 is mainly used to calculate electric fields based on electrode formations with specified voltages, as well as to simulate the trajectories of charged particles under various conditions, including RF effects, magnetic fields, and collisions. More details about this software can be found in the printed SIMION manual, additional electronic literature, and various resources available on the SIMION.com website. To our knowledge, no earlier research has investigated the effect of third electrode geometry on the transmittance of the electron beam and the cross-over radius of the paraxial trajectory using SIMION simulations.

2. Geometrical Design and Calculation Procedure

A key requirement for ES lenses is that they operate within a well-maintained vacuum environment to minimize the risk of electrical discharge and system failure. In the past, personnel adopted a numerical computer program that utilized the electrode geometry in either rectangular or cylindrical coordinates to calculate electric potential and field distribution. In this study, the proposed lens was designed using SIMION8. The computations included the axial field, potential distribution, and equipotential lines. A LUA program was used to determine the trajectory of the electron beam and emittance parameters [10]. Figure 2 shows the design of the Einzel lens, which comprises three electrodes. Two electrodes have both a potential of V_1=0 volts, and the central electrode has a potential of V_2=10 volts. The first and second electrodes have identical dimensions (10 x 3 mm), and the third electrode has dimensions of 3 × 3 mm.

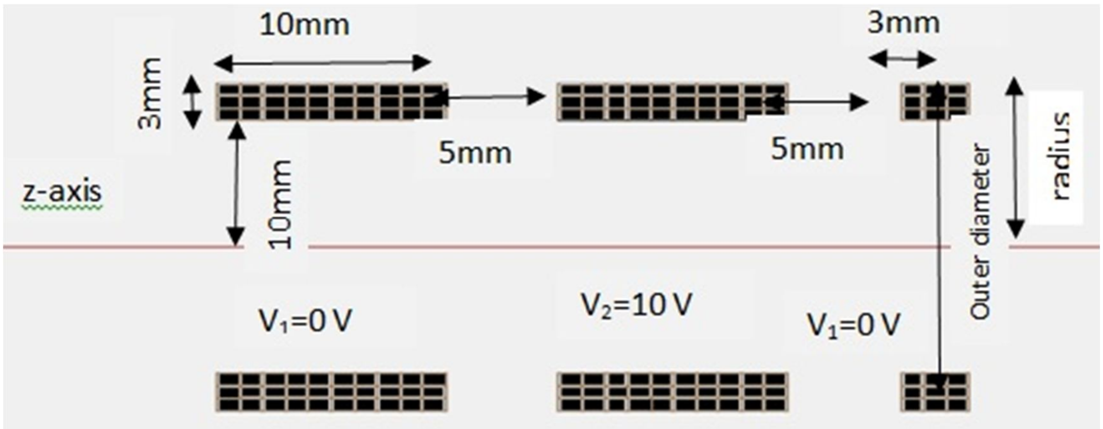

FIG. 2. Cross-sectional representation displaying the configuration and size proportions of a tripolar Einzel lens.

The axial electric field distribution is simulated after creating the electrode geometry and completing the electrical configuration of the lens. The Laplace equation is solved to determine the potential values and establish the boundary conditions, following Gauss's theorem as described by the equation:

$$\nabla.\vec{E} = 0 \qquad (3)$$

The axial electric field distribution is calculated using numerical techniques, specifically the finite difference method (FDM). This entails selecting the electric field values through Poisson's equation and calculating the electron beam paths (r) using Lorentz's and Maxwell's equations [11]:

$$\nabla.E = \frac{\sigma}{\varepsilon_o} \qquad (4)$$

$$\vec{F} = G(\vec{E} + V \times \vec{B}) \qquad (5)$$

where E is the electric field, σ is the charge density, ε_o is the vacuum permittivity, and B is the magnetic field (set to 0).

Electrostatic fields are treated as solutions to the boundary value problem of Laplace's equation using FDM within SIMION 8.0. The trajectory of the electron beam and the emittance parameters are then computed using a LUA program that employs the Monte Carlo numerical method [12].

The structured steps for optimizing the third electrode are organized as follows:

2.1 Effect of Increasing the Outer Diameter of the Third Electrode

Figure 3 depicts the distribution of equipotential surfaces within the lens. The figure shows how these surfaces change as the outer radius of the third electrode varies (R = 13, 16, 19, 22, 25, and 28 mm). Increasing the diameter of the third electrode (iron material = 18 mm) reduces flux leakage from the lens toward the electron beam exit, compared to a smaller electrode diameter (iron material = 3 mm). This contrast results in a growing intensity of the flux lines within the lens as R increases. This, in turn, leads to a special behavior of the electron beam within the lens, ultimately impacting the path and emittance of the electron beam. This characteristic will serve as a conclusive factor in determining the additional optical properties of the Einzel lens [7]. Figure 4 shows a contrast between the axial electric field and the distribution of electric potential, calculated for different outer radius values of the third electrode (R) as a function of the z-axis. This graph illustrates the axial field distribution of an Einzel lens, where the middle electrode has a higher voltage than the two outer electrodes. Notably, the potential distribution V(z) stays constant at the boundaries, and the electric field E (z), given by the first derivative V′(z), where $E = -\nabla V$, is zero. This observation suggests the absence of an electric field outside the lens, creating a region without a field that spans from the lens terminals. In this region, the trajectory of charged particle beams remains straight due to the absence of any external forces acting upon them [13].

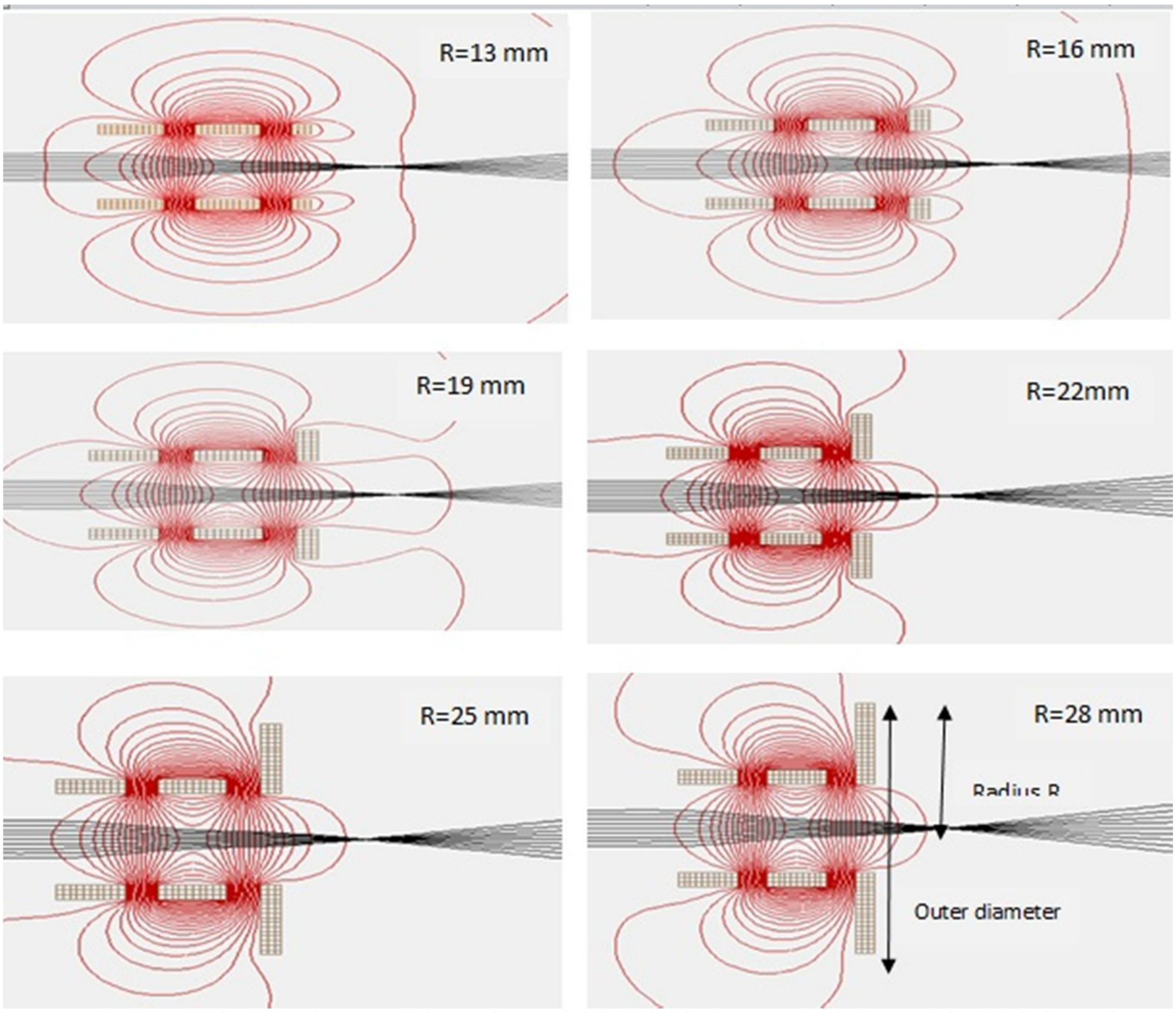

FIG. 3. Changes in the trajectory of the equipotential lines with the outer radius (R) of the third electrode. Increasing the electrode's iron material to 18 mm reduces leakage.

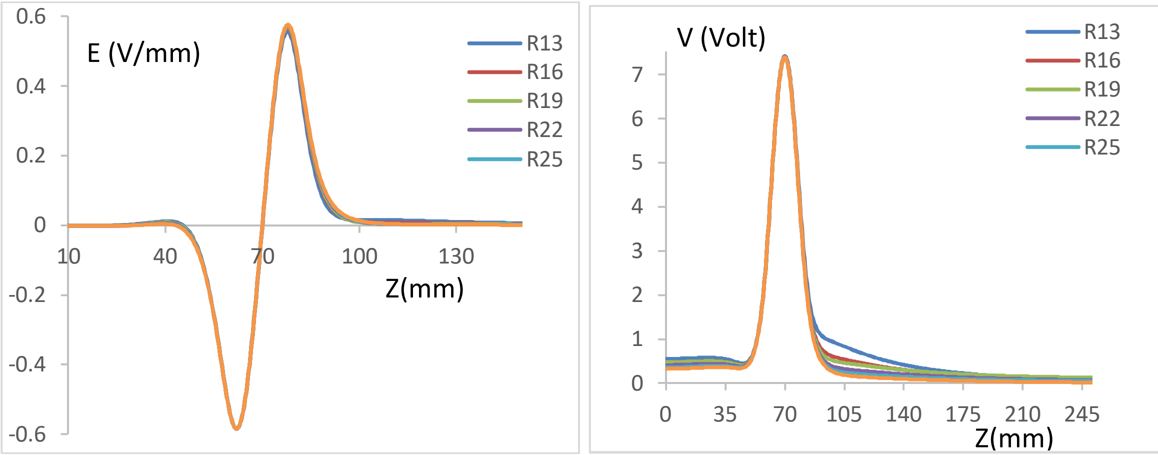

FIG. 4. Differences in the electric field (E) and axial potential distribution (V) along the z-axis for various radius values (R = 13, 16, 19, 22, 25, and 28 mm).

The electrons' trajectories (r) are plotted in Fig. 5, illustrating the disparity of the electron beam path (r) with outer radius (R) as a function of Z. The figure shows that increasing the outer radius of the third electrode improves the electron trajectories and reduces the radius at the focal point. Also, the path of the electron beam and emittance are plotted in Fig. 6 as a function of outer radius (R). From this figure, it is evident that the outer radius of the third electrode (R=19 mm) has a better focal length point (r =0.039 mm) and lower emittance (Ɛ=2.839 mm.rad). So, increasing the outer radius of the third electrode and controlling the stray electric equipotential lines outside the lens represent significant advancements. These discoveries open new oppor r (mm) achieving higher beam quality, precision, and efficiency in charged particle optics applications.

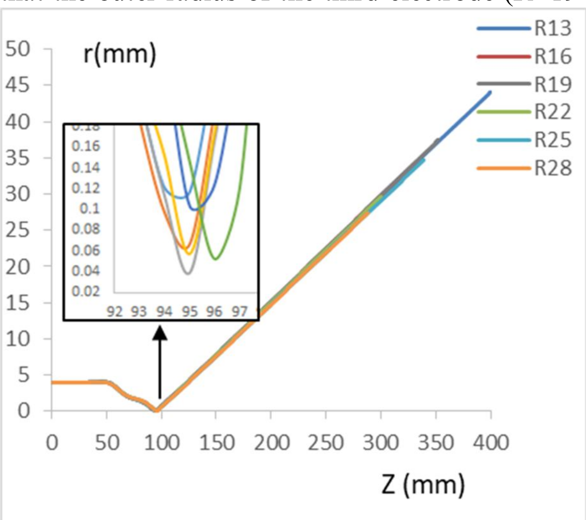

FIG. 5. The path of the electron beam (r) with respect to the z-axis for varying values of R.

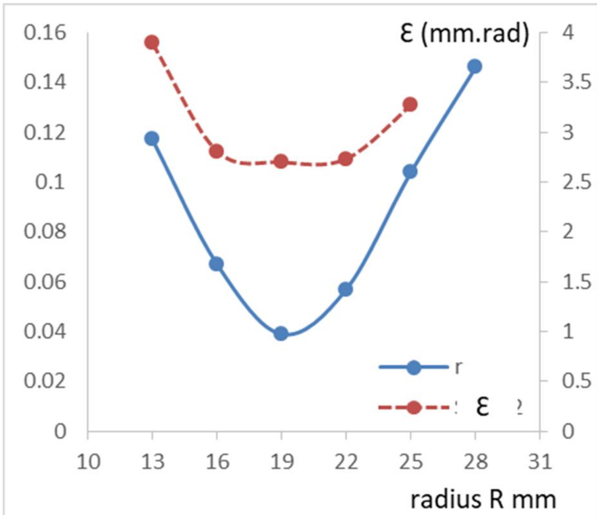

FIG. 6. The path of the electron beam (r) and emittance Ɛ as a function of radius R.

2.2 The of Effect Third Electrode Length

In the present study, we adopted a cylindrical shape for the third electrode, serving as a cover for the first and second electrodes, and investigated the impact of increasing its length. The effect of extending the cylindrical third electrode (S) was analyzed for the optimal lens configuration identified in the previous section (R = 19 mm). Figure 7 illustrates the changes in the equipotential field distribution within the lens as the electrode length increases (S = 5, 10, 15, 20, 25, and 30 mm). It is evident that lengthening the cylindrical third electrode reduces flux leakage and increases the density of flux lines inside the lens. This results in a more regular distribution of the equipotential lines, leading to improvements in the paraxial ray trajectory as well as in the shapes of the electric field and electric potential distribution curves, as shown in Fig. 8.

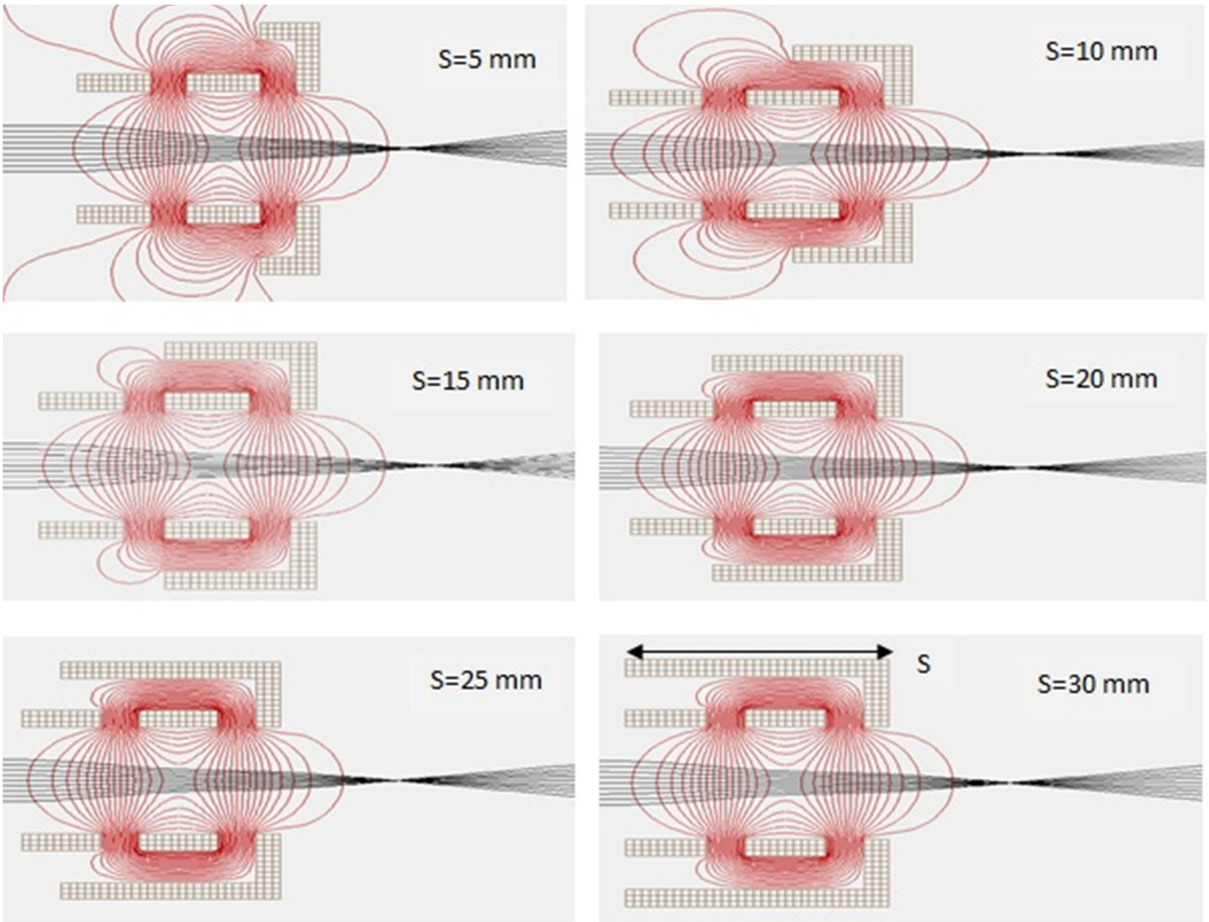

FIG. 7. Changes in the trajectory of equipotential lines with variations in the length of the third electrode (S = 5, 10, 15, 20, 25, and 30 mm).

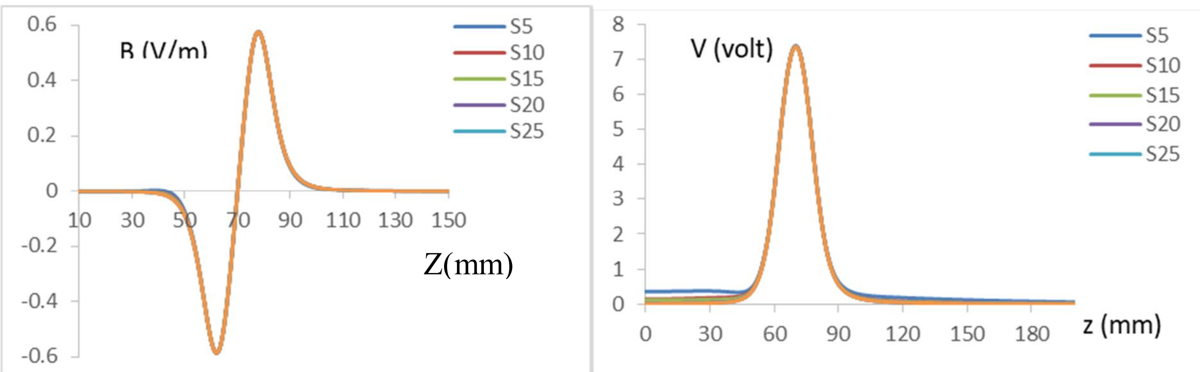

FIG. 8. Differences in the electric field (E) and axial potential distribution (V) concerning the z-axis for different values of the third electrode length (S = 5, 10, 15, 20, 25, and 30 mm).

The trajectory of the electron beam through the designed lens at different S values along the z-axis is depicted in Fig. 9. The figure demonstrates that as the length of the third electrode value increases (S = 25 and 30 mm), the gradient of the electron beam's path decreases. This results in an improved path of the electron beam and a reduction in the focal point diameter. Figure 10 shows the electron beam path (r) and the beam emittance (Ɛ) as a function of the third electrode length (S). Both parameters drop significantly at S=25 mm. These results indicate that the third electrode's cylindrical shape, which encapsulates the first and second electrodes, outperforms the traditional cylindrical design. This innovative configuration provides superior beam control and focusing capabilities, leading to enhanced lens efficiency.

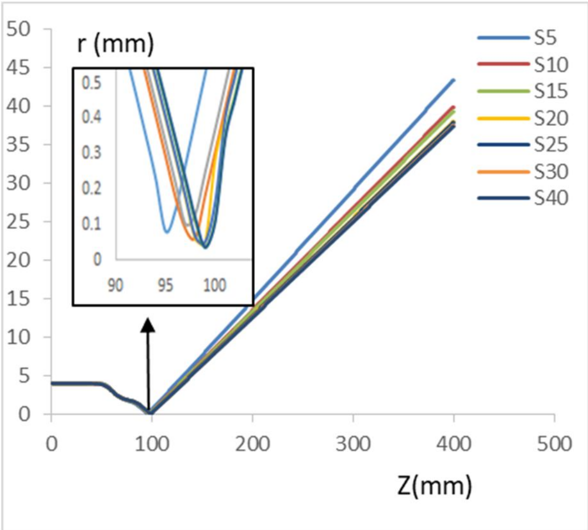

FIG. 9. The electrons' trajectories as a function of the z-axis for different values of length S.

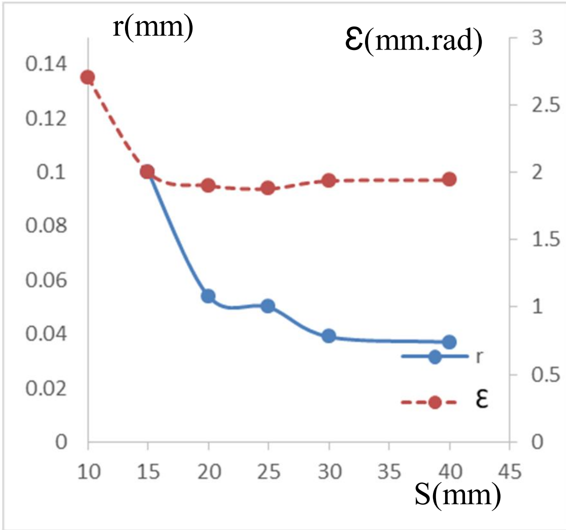

FIG. 10. The path of the electron beam (r) and emittance Ɛ as a function of length S.

2.3 The Length of the Electron Path within the Third Electrode

The initial beam particles' arrangement is created to observe their motion when projected paraxially with an initial energy from a distant source. This process provides insight into the optical characteristics of the electrodes making up the lens [14]. In this research, the effect of the length of the electron path within the third electrode was studied for various values of the length (L=2, 4, 6, and 8 mm). Figure 11 shows the distribution of the equipotential surface of the lens at values of L= 2, 4, 6, and 8 mm, radius R=19mm, and the length of the third electrode S= 30 mm. We can see that increasing the electron path length within the third electrode does not affect the distribution of the equipotential surfaces. Thus, the distributions of the field (E) and the electrical potential (V) are not affected, as illustrated in Fig. 12.

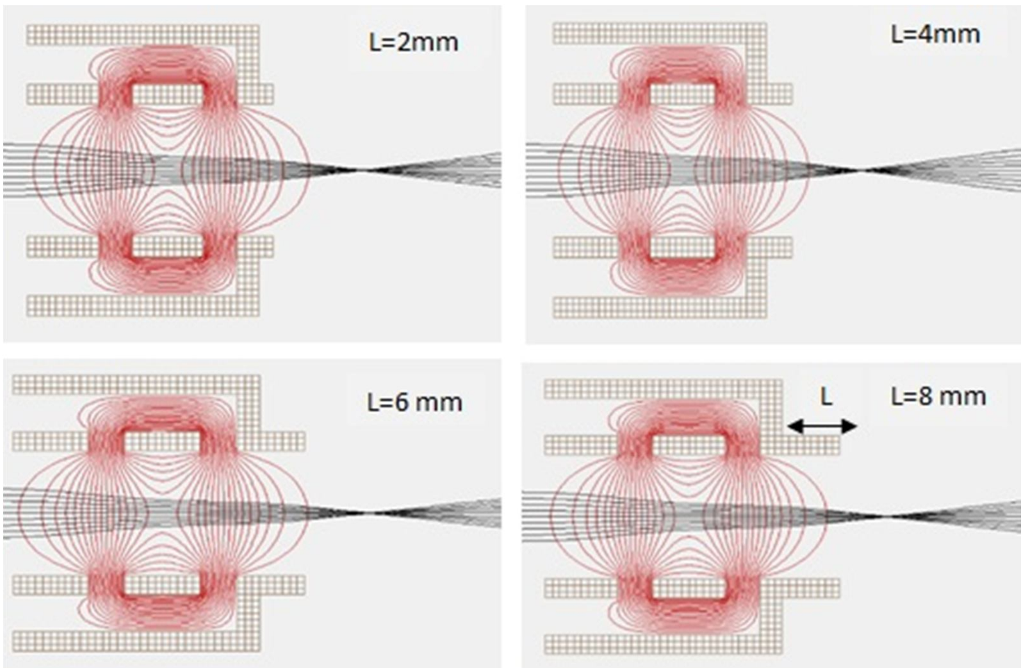

FIG. 11. The equipotential lines trajectory with variation of the length of the electron path within the third electrode (L = 2, 4, 6, and 8 mm), at constant value of R = 19mm & S = 30mm.

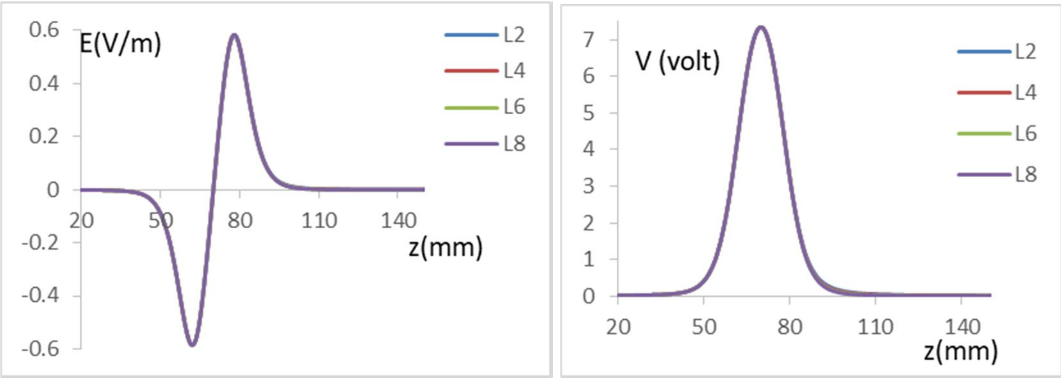

FIG. 12. Differences in the electric field (E) and axial potential distribution (V) along the z-axis for varying lengths of the electron path within the third electrode (L).

Figure 13 depicts the trajectory of the electron beam (r) within the lens at various lengths of the electron pathway inside the third electrode (L) along the z-axis. It is clear from this figure that increasing the length of the electron path with the third electrode length (L), produces a drop in radius of the focal point, reaching r = 0.065 mm at L = 6 mm. This increase in L also causes reduced beam emittance, as shown in Fig. 14, where the emittance decreases to Ɛ = 1.94 mm.rad. The electrostatic lens aberrations depend on the path taken by charged particles, and these aberrations are minimized when the particle trajectory is shorter. Furthermore, it was observed that the length of the electron beam's path within the third electrode has a scant impact on the propagation of the electron beam. The primary influence on the overall trajectory comes from other parameters.

Figure 15 illustrates the eventual configuration of the electrostatic Einzel lens and its optimized measurements. This depiction presents a 3D representation of the supplemented design of the third electrode of the electrostatic Einzel lens.

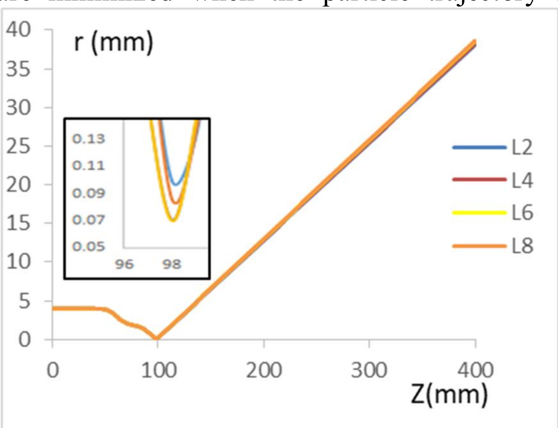

FIG. 13. The electron beam path (r) as a function of the z-axis for different values of L.

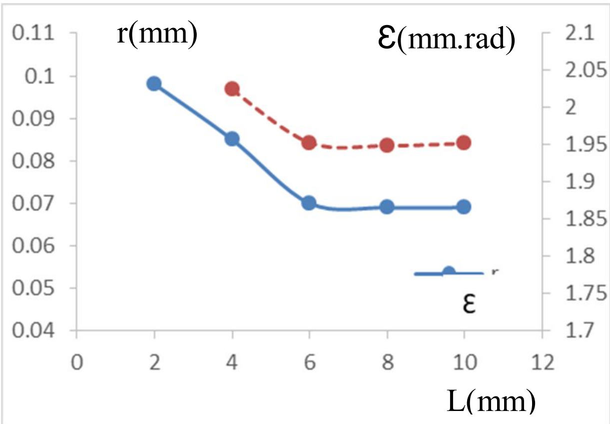

FIG. 14. The electron beam path (r) and emittance Ɛ as a function of L.

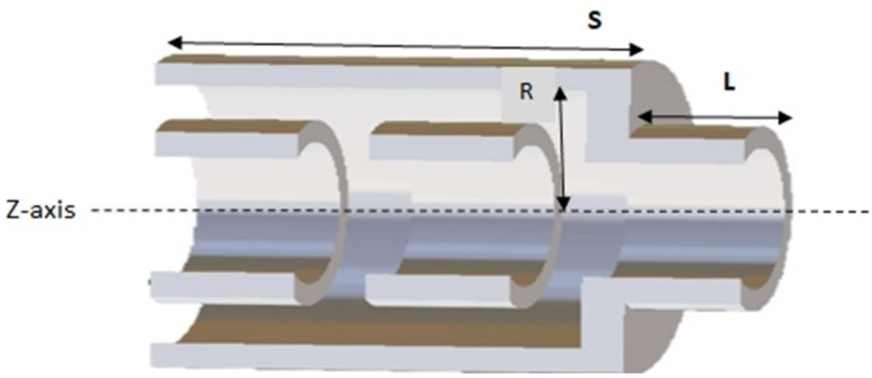

FIG. 15. Three-dimensional visualization of the finalized design of the proposed third electrode.

3. Results and Discussion

This investigation has made significant progress in designing various electrostatic lenses, with remarkable functioning enhancements. Through an overall exploration of parameters, such as the outer diameter and length of the third electrode, as well as the length of the electron path within the third electrode, we have achieved substantial improvements in lens properties.

3.1 The Effect of Increasing the Outer Diameter of the Third Electrode

A key finding of this study is that the existence of stray electric equipotential lines outside the Einzel lens impacts electron beam emittance and beam radius negatively. To reduce leakage of the electric flux towards the exit of the lens, the diameter of the third electrode must be increased. These improvements include a reduction of beam emittance values by 73% and a decrease in the cross-over radius of the paraxial trajectory by 27%. This highlights the decisive role of proper design and electric field shaping within the lens to achieve optimal performance.

3.2 The Effect of Third Electrode Length

Furthermore, the results suggest that the third electrode's cylindrical shape, which encapsulates the first and second electrodes, outperforms the traditional cylindrical shape. Increasing the length of the iron material of the third electrode limits flux leakage outside the lens. High density and regularity of flux lines optimized the paraxial ray trajectory by 37%, and reduced emittance by 76%. This creative configuration provides superior beam control and focusing capabilities, leading to enhanced lens efficiency.

3.3 The Length of Electron Path within the Third Electrode

Finally, it was noted that the length of the electron ray within the third electrode has a limited impact on the propagation of the electron beam from the lens. While the overall trajectory is mainly affected by previous parameters, this factor contributes to a more complete understanding of the electron beam's behavior within the lens system. As such, this research contributes to the development of cutting-edge technologies in various fields involving electron and ion beam systems, particle accelerators, and advanced microscopy.

Acknowledgment

I would like to express my thanks and appreciation to the University of Mosul, Iraq, for its valuable support and contributions to the completion of this research. I also appreciate the academic guidance provided by the university staff, and I extend my thanks to everyone who contributed to this study.

References

[1] Hinterberger, F., "Ion Optics with Electrostatic Lenses", Helmholtz-Institut für strahlem-und Kernphysik, (University of Bonn, Germany, 2005).

[2] Alsheikh Essa, A.A., Kheder, K.Q., and Alabdullah, A.I., "An Investigation of the Link between Radius and Energy Resolution Capability in Hemispherical Electron Energy Analyzer", (2023), Under publication.

[3] Kanaan, M.I., Alabdullah, A.I., and Al-Ahmad, A., Rafidain J. Sci., 32 (2) (2023) 30.

[4] Ahmad, A.A., Rafidain J. Sci., 25 (3) (2014) 70.

[5] Rashid, M.H., Proc. DAE Symp. Nucl. Phys., 56, (2011).

[6] Sulaiman, M.I., M.Sc. Thesis, University of Mosul, (2022), Iraq.

[7] Abdullah, R.T. and Hussein, O.A., J. Phys.: Conf. Ser., 1530 (2020) 012128.

[8] Hawkes, P. and Kasper, E., "Emittance, Principles of Electron Optics", 2nd Ed., (Sciencedirect.com, 2018),

[9] Jaechung, K., "Beam emittance", (Department of Nuclear Engineering, Seoul Natianal university, 2017),

[10] Alabdullah, A.I.M., Optik, 268 (2022) 169761.

[11] Halliday, D. and Resnick, R., "Fundamentals of Physics", 10th Ed., Extended Ed., (QC21.3.H35, book, 2014).

[12] Kanaan, M.I. and Alabdullah, A.I., Rafidain J. Sci., 32 (3) (2023) 55.

[13] Al-Ani, M.M., M.Sc. Thesis, College of Science of Al-Nahrain University, Baghdad, (2007), Iraq.

[14] Li, C., Huang, W., Du, Y., Yan, L., and Tang, C., Proc. IPAC, San Sebastian, Spain, (2011).